*32nd EPS Conference on Plasma Phys. Tarragona, 27 June - 1 July 2005 ECA Vol.**29C**, P-5.008 (2005)*

High-Density Deuterium Plasma Discharge in NAGDIS-II with Double Anode Configuration

Dai Nishijima, I. Yagyu, M. Takagi, N. Ohno and S. Takamura
Nagoya University, Nagoya, Japan

1. Introduction

The plasma density of the divertor plasma in ITER is expected to be an order of 10^{19} m^{-3} or more. However, the plasma density in the linear divertor plasma simulator NAGDIS-II is not so high compared with that of the divertor plasma, especially for hydrogen isotopes plasma. NAGDIS-II is mainly consisted of the plasma source region and the divertor test region, and maximum electron density of deuterium plasma at the divertor test region so far is early 10^{18} m^{-3}, which is limited by instability of discharge. The voltage of direct-current (DC) discharge increases and begins to fluctuate as the discharge current increases, and finally the discharge disappears. In order to stabilize the DC discharge and to obtain high-density deuterium plasma targeted on an order of 10^{19} m^{-3}, the second auxiliary anode is placed in NAGDIS-II. The structure of the second anode is hollow type, the same as the first one. Such an anode structure increases the effective surface of anode and decreases the conductance between the plasma source region and the divertor test region. We expected that a reduction of neutral gas pressure in the test region could increase plasma density because it decreases the rate of charge exchange process between deuterium ion and neutral gas. This paper shows some initial experimental results of the double anode configuration and offers indications for optimizing the deuterium plasma discharge in NAGDIS-II.

2. Experimental set-up

Figure 1 shows the schematic of NAGDIS-II with the second anode (Anode-II). NAGDIS-II is the cylindrical device with a length of ~3.0 m and a diameter of ~0.2 m, which produces low-temperature plasma in steady state by DC arc discharge. The device is composed of mainly three regions, the plasma source region, inter-anodes region and the divertor test region as shown in Fig.1. A thermo-electron emitter LaB_6 disk 108 mm in diameter is placed in a molybdenum cathode container with an aperture 30 mm in diameter. A cusp magnetic field is formed in front of the LaB6 disk in order to squeeze the emitted electrons. An

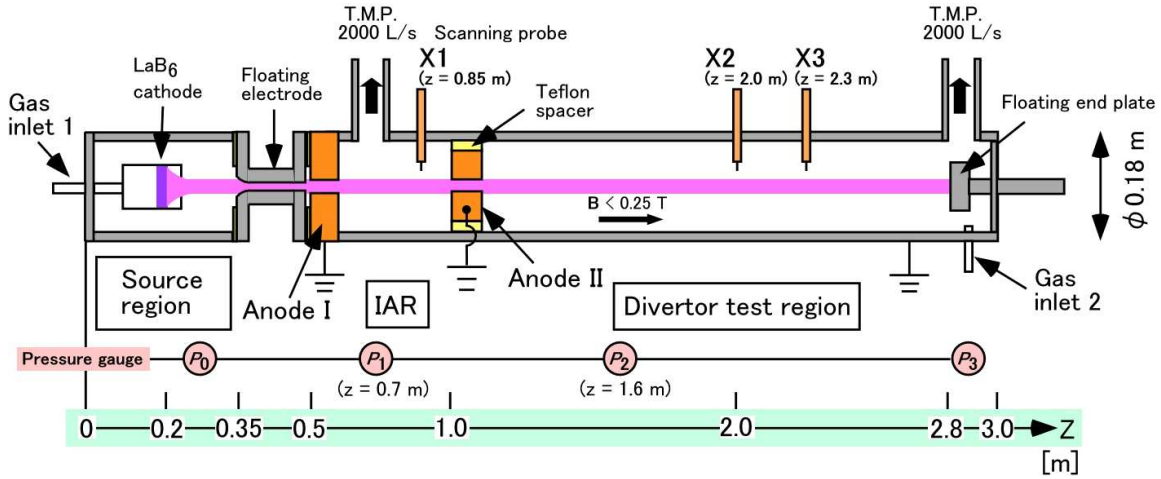

Fig. 1 Schematics of NAGDIS-II with two anode of Anode-I and Anode-II.

intermediate hollow electrode (floating electrode) with the hollow diameter of 20 mm and the tube length of 180 mm is put between the cathode and the first anode (Anode-I). The vacuum chamber is electrically grounded and the potential of the Anode-I is also set in the ground potential. The intermediate electrode is electrically floating, in other word, insulated from the vacuum chamber and the Anode-I. The diameter and the tube-length of Anode-I is 24 mm and 60 mm, respectively. The neutral gas pressure in the test region can be kept to less than 1 mTorr due to a low gas conductance of the floating electrode and two 2000 L/s turbo-molecular pumps equipped at the both ends of the test region, while the gas pressure in the source region is more than 100 mTorr. Gas pressure in the chamber is measured by four vacuum pressure gauges (P_0 -P_3) at different points as shown in Fig. 1. Three scanning triple probe systems, X1 (z = ~0.9 m), X2 (z = ~2.0 m) and X3 (z = ~2.3 m) gain radial distribution of plasma parameters. 21 solenoidal magnetic coils not shown in Fig. 1 produce the axial magnetic field up to ~ 0.25 T in axial direction according to the magnetic coil current.

Figure 2 shows a photograph of the Anode-II made of copper, which has a hollow in the centre with the diameter of 27 mm and the tube-length of 62 mm. This anode is also water-cooled type,

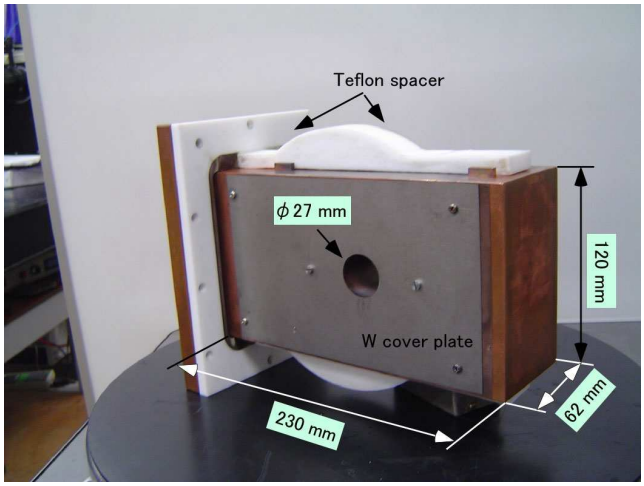

Fig. 2 Schematic of Anode-II.

the same as the Anode-I. The both sides of anode surface are covered with tungsten (W) plates in order to prevent an ion sputtering. The Anode-II is placed at the position of z = ~1.0 m, which is ~0.4 m away from the Anode-I. The gaps between the chamber wall and the rectangular Anode-II are filled in with Teflon spacers as shown in the Fig. 1 and Fig. 2, which make the
Anode-II electrically isolated from the chamber. The potential of Anode-II is, however, set at the same as that of the chamber (ground potential) in this experiment. The electrical isolation of the Anode-II is for the future work that investigates the dependence of the potential of Anode-II for plasma discharges, which is not treated in this paper. In this paper, we call Single Anode Configuration (SA-C) for the old configuration without the Anode-II, while the new configuration with the Anode-II is called as Double Anode Configuration (DA-C). The region between anodes is called as Inter-Anode Region (IAR). In addition, some physical notation used in this paper are as follows: discharge current between anodes and cathode I_{dis}, discharge voltage V_{dis}, electron density n_e, electron temperature T_e, plasma space potential V_p, gas flow rate of gas inlet at the source region Gas_{in1}, gas flow rate of gas inlet at the test region Gas_{in2}, neutral gas pressure at each vacuum gauge $P_{0,1,2,3}$, magnetic field coil current I_{mag}, magnetic field strength B, axial position z and radial position from the centre of the plasma column r.

3. Experimental results and discussion

Deuterium discharges in SA-C1 and DA-C1 with the common experimental conditions of Gas_{in1} 80 sccm, I_{dis} 20 A and I_{mag} 200 A(~0.1T) are compared. Figure 3 (a) and (b) show the radial profiles of n_e in SA-C1 and DA-C1 measured by the probes at X1, X2 and X3. The gas pressure P_3 decreased from 0.4 mTorr of SA-C1 to 0.1 mTorr in DA-C1. However, n_e in the test region was drastically decreased contrary to our expectation and was about tree times less than that of SA-C1. What is worse was that V_{dis} increased to 160 V in DA-C1 from 145 V of SA-C1. These results indicate that mere setting the Anode-II has unfavourable effects on the plasma production in the test region that n_e decreases and V_{dis} increases.

The problems made a change for the better when the gas pressure in the test region was increased by gas puffing at the gas inlet 2. Figure 3 (c) shows n_e profile in DA-C2 with a Gas_{in2} of 100 sccm and other conditions were the same as those of DA-C1. This gas puffing increased P_3 to 1.8 mTorr and also boosted n_e at the test region to approximately ~1 x 10^{18} m^{-3}. V_{dis} decreased down to 125 V. This result

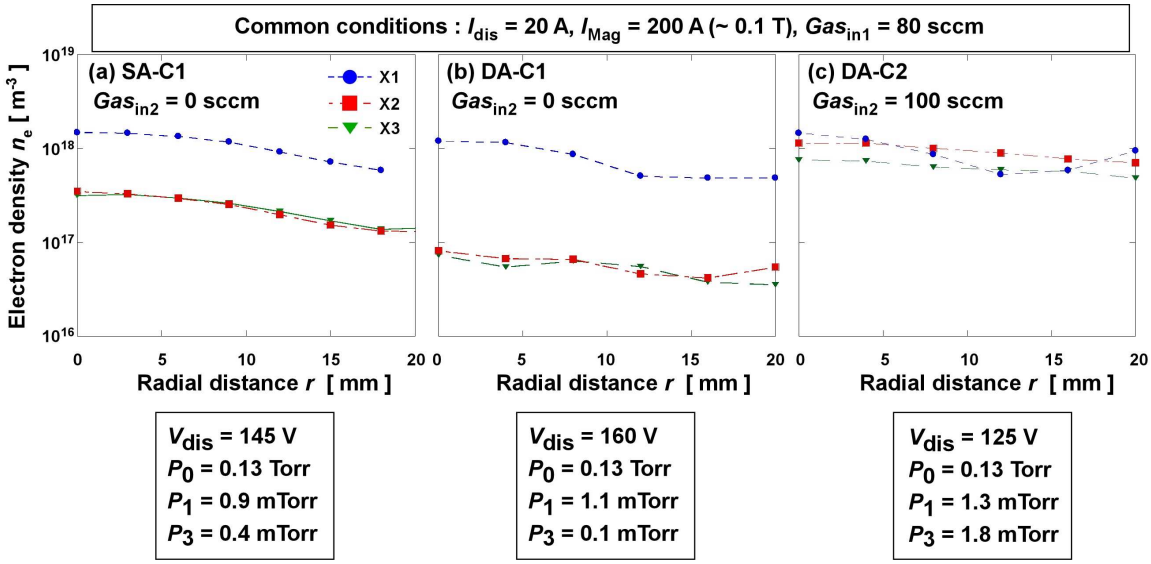

Fig. 3 Radial profiles of electron density n_e in three configurations of SA-C1, DA-C1

indicates that an amount of gas pressure in the test region is necessary to obtain high-density deuterium plasma. Gas puffing at the test region decreased V_{dis} and stabilized the discharge, which enabled to expand the limit of I_{dis} from ~80 A to 160 A. Figure 4 (a) shows the dependence of I_{dis} for n_e at the centre of radial position (r = 0) measured at X1, X2 and X3 with conditions of Gas_{in1} = 80 sccm and Gas_{in2} = 80 sccm. The n_e increased approximately proportional to I_{dis} in all the probes and close to the order of 10^{19} m^{-3} (Fig. 4 (a)). T_e at all the probes were less than 10 eV and V_{dis} was kept at almost constant value of around 125 V. Gas pressure at source region P_0 also increased as the I_{dis} increased due to the plasma plugging effect, while gas pressure at the test region P_1 and P_3 exhibited steady state characteristics as shown in Fig. 4 (c). Although there were unexpected phenomena, the initial target of increasing n_e was achieved due to the second anode and gas puffing in the test region.

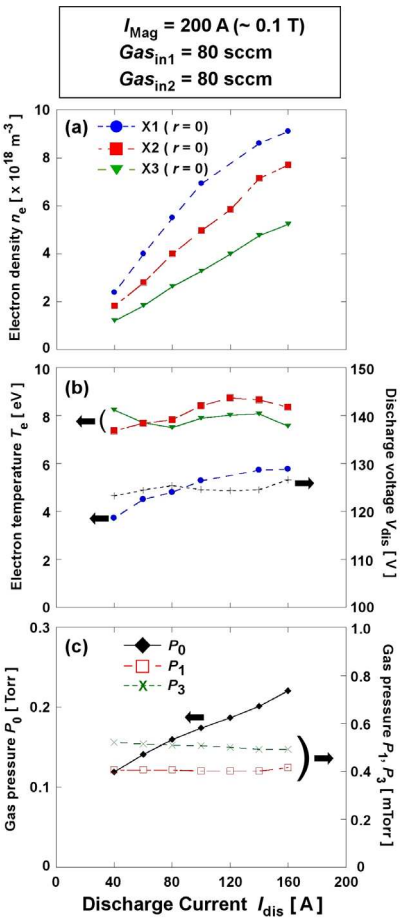

Fig. 4 Dependence of discharge current I_{dis} for (a) central density of each probes, (b) electron temperature T_e and discharge voltage V_{dis} and (c) gas pressure at each vacuum gauge.